JOURNAL OF MATERIALS SCIENCE 3 (1968) 244–258

Defects and Laser Action in GaAs Diodes

M. J. HILL, D. B. HOLT
Department of Metallurgy, Imperial College, London SW7, UK

Received 20 November 1968

Zn-diffused, Te-doped GaAs injection lasers were examined by means of infrared microscopy, etching, transmission electron microscopy and scanning electron probe microanalysis.

Bands of high infrared absorption, i.e., striations, were present in many diodes and the lines of intersection of the striations with the p-n junction were minimum emission filaments. Misfit dislocation networks were present in the p-n junction region but did not influence the emission pattern. Precipitates and diffusion-induced dislocations were found in the zinc-diffused region. All the properties of the material that enter into the expression for the threshold current for laser action were considered. It was concluded that the striations affect laser emission patterns mainly through the variation of the infrared absorption coefficient.

1. Introduction

GaAs injection laser diodes emit non-uniformly [1-3]. That is to say, as the forward current through the p-n junction is increased through threshold, first one, and then more and more bright spots appear along the line of intersection of the p-n junction with the Fabry-Perot mirror face. These spots emit coherent radiation.

The yield of diodes exhibiting laser action and the performance of these diodes is known to vary with the material preparation techniques employed. Therefore it seemed worthwhile to examine the defect structure and the distribution of chemical impurities in GaAs laser diodes, and to attempt to correlate these with what has become known as spotty laser action.

Non-uniform laser action has been found in GaAs diodes whether the n-type dopant was Te, Se, or Si, and in diodes prepared both by diffusion and by epitaxial deposition from Ga melts. A variety of different types of defects may therefore play a role in producing spotty laser emission. In order to obtain a complete picture of the non-uniformities in GaAs lasers, it is necessary to employ a number of different methods of observation. Results obtained by employing emission and transmission infrared microscopy, etching, transmission electron microscopy, and electron probe microanalysis are presented in this paper.

2. Experimental Methods

The equipment used for the infrared optical study of the lasers is shown in fig. 1. The vacuum cryostat and associated circuitry were built to designs developed by workers at the Services Electronics Research Laboratory*, who also kindly supplied the GaAs laser diodes that were examined. The pulse generator produced 10 to 1000 square pulses/sec, each of length 5μsec. The pulses were fed to the pulse forming line. The pulse heights were varied from 0 to 240 A by altering the power from the DC supply. The current pulse heights were monitored by one beam of the oscilloscope which was triggered by the generator, and was connected across a 0.1 Ω resistance in the pulse-forming circuit. The intensity of the light pulse from the laser was monitored by the second of the oscilloscope beams, which was connected across a 1 Ω resistance in series with the silicon solar cell.

For infrared photomicrography, Kodak IR-ER plates were used. In order to examine the defect content of the p-n junction and of planes parallel to it in the Zn-diffused p-type region, a

*Address: Baldock, Herts, UK

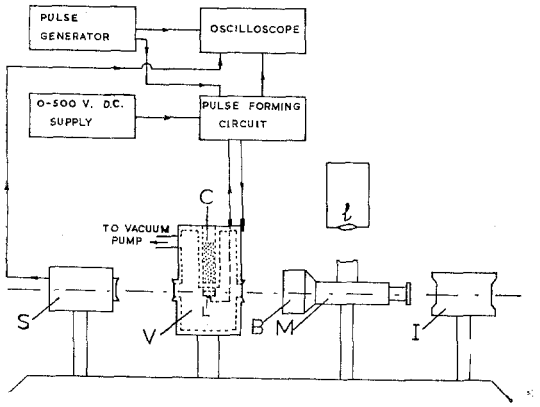

Figure 1 Laser equipment. *C* is a cold (liquid N_2) finger in a vacuum cryostat, *V*, containing the Laser, *L*. *S* is a silicon solar cell for measuring the intensity of the infrared emission from one face of the laser, the other face of which may be observed by means of a microscope *M* fitted with a Burch long working distance reflecting objective, *B*, and a lamp for reflection illumination, *I*. The emission was observed by means of an infrared image converter *I*, for which a camera could be substituted for photomicrography. For transmission infrared microscopy an incandescent lamp was substituted for the silicon solar cell.

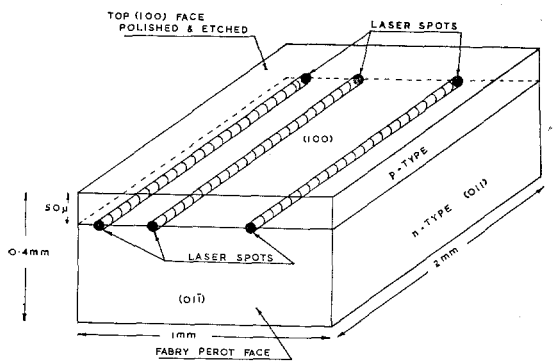

Figure 2 Orientation and dimensions of GaAs laser diodes.

technique of successive chemical polishing and etching was developed. Polishing by means of bromine-in-methanol solutions was employed with the rotating beaker method, to produce smooth faces parallel to the p-n junction at successive depths in the p-type material, as indicated in fig. 2. Measurements showed that the rate of removal of material by bromine in methyl alcohol varied as shown in fig. 3. It was possible, therefore, by using a 0.125% Br_2 solution for 5 to 10 min to examine successive planar sections parallel to the p-n junction spaced a few microns apart. The GaAs diodes were mounted in North Hill Metallurgical Mounting Plastic to prevent attack on the bottom and side faces. The successive polished faces were etched by immersion for 2 min in Abrahams' and Buiocchi's AB reagent, held at room temperature [4].

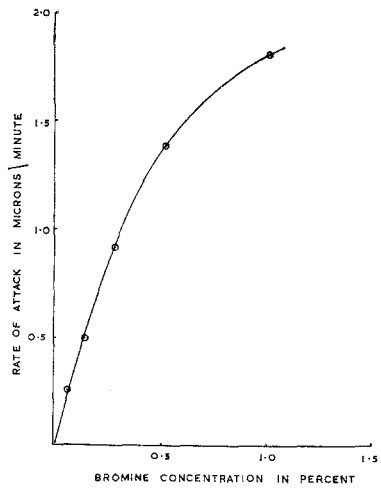

Figure 3 Variation of attack rate with composition for bromine in methyl alcohol polishing of GaAs.

Electron probe microanalyser observations were made in a Cambridge Instruments Geoscan analyser, and in a JEOL microanalyser. In each case the observations were made on faces parallel to the p-n junction, prepared either by polishing, or by polishing and etching, as just described. In order to prevent electrostatic charging effects the face to be examined had a layer of carbon evaporated on to it before insertion into the microanalyser.

Specimens were thinned for examination by transmission electron microscopy using the chemical jet polishing technique [5]. However, it was found that due to operator error, frequently no electron transparent area was obtained. Equipment was therefore developed in which a photomultiplier signal, which occurred when the GaAs became optically transparent, was amplified and fed to a relay which pulled the specimen out of the jet of chemical polish [6].

3. Results

3.1. Infrared Micrography

By micrographing the front and back mirror faces of a number of lasers, it was established that the spots appeared in matched pairs at the ends of lines or filaments running perpendicularly to the Fabry-Perot mirror faces. It was also found in all cases that the spot pattern in any

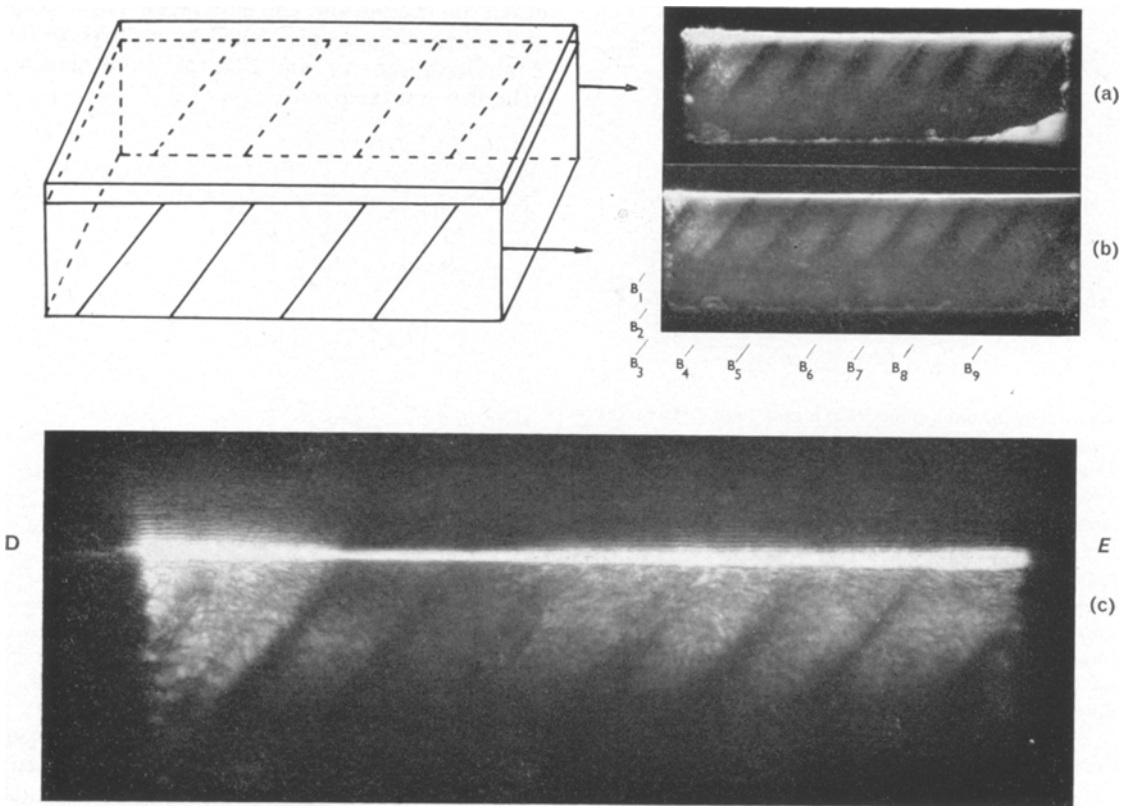

Figure 4 Micrographs of infrared emission from diode 2659/5 with 80 A, 5μsec pulses flowing through it and using a 10 sec exposure (a, b), and with 80 A flowing and using a 5 sec exposure (c). These are the near-field radiation patterns, i.e. the microscope was focused on the front (01$\bar{1}$) face of the diode in (b) and (c), and on the back face in (a). The dark bands, *B*, intersect the p-n junction at points of minimum width of the bright emission line. This is best seen by viewing micrograph (c) along the line of the p-n junction from *E* to *D*. (Micrograph (a) was reversed in printing.)

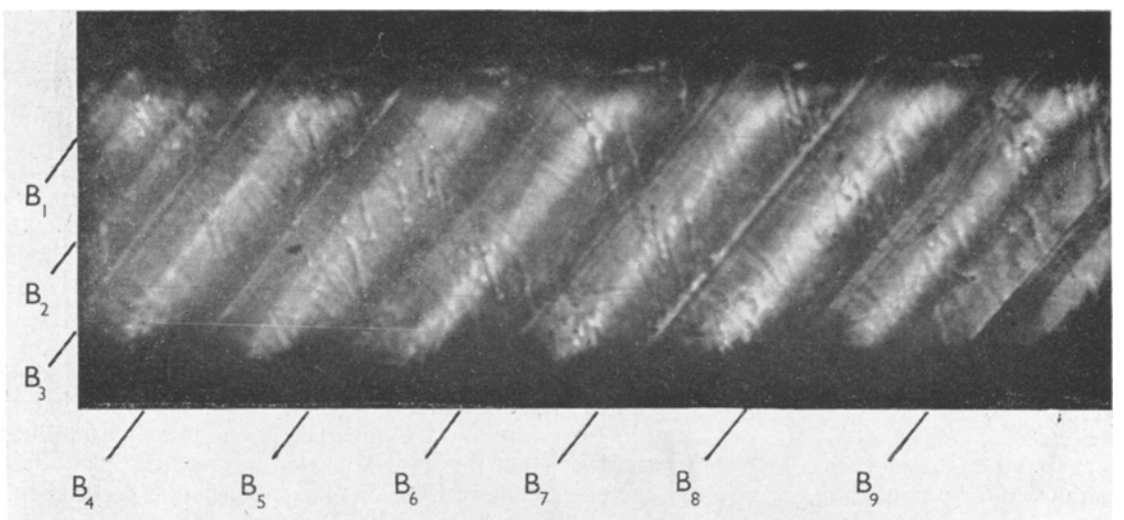

Figure 5 Transmission infrared micrograph of the face shown in fig. 4c.

diode was reproducible. That is, on turning the current up through threshold, the spots always appeared in the same places and in the same sequence. There is, therefore, a fixed pattern of favoured laser filaments in the region of the p-n junction. The pattern is fixed both in position in the diode, and in the critical value of the total diode current at which each filament begins to lase.

No defects on the polished front or back mirror faces of the diodes, $(0\,1\,\bar{1})$ or $(0\,\bar{1}\,1)$ (fig. 2), such as polishing scratches were found to correlate with emitting spots.

A micrograph of the infrared emission from diode 2659/5 operated well above the threshold for laser action is shown in fig. 4c. This is a near-field radiation pattern, i.e. the microscope was focused on the front emitting face of the diode. A number of laser spots were active at the large value of diode current, giving an impression of nearly continuous emission, but with varying intensity, along the p-n junction.

Dark bands running diagonally through the infrared transparent n-type GaAs appeared in long exposure (10 sec) and high current infrared emission micrographs of a number of diodes as, for example, can be seen in fig. 4c. The points of intersection of these bands with the p-n junction were points of minimal emission. At lower values of diode current it could be seen that these positions were those separating active laser spots.

By photomicrographing both the front and the back mirror faces in emission, it was established that matching pairs of dark bands appeared at the lines of intersection of particular $(1\,\bar{1}\,\bar{1})$ planes, with the front and back surfaces of the diodes, as shown in figs. 4a and b.

Viewed in transmission, a considerable internal structure of sharp parallel lines could be seen in the dark bands, as is shown in fig. 5. In general, there is a central line in the bands, flanked by pairs of equidistant lines, as is most clearly visible in bands B_3, B_6 and B_8. In addition, dots and blobs can be seen, many of them aligned in apparently random directions.

Optical inhomogeneities are often not as regular as those shown in fig. 5 (which were typical of all the diodes produced from one single crystal). Even when the inhomogeneities were less regular, however, they sometimes correlated with the emission pattern, as shown in fig. 6. Fig. 6a is a transmission infrared micrograph showing curved and irregularly spaced striations, and

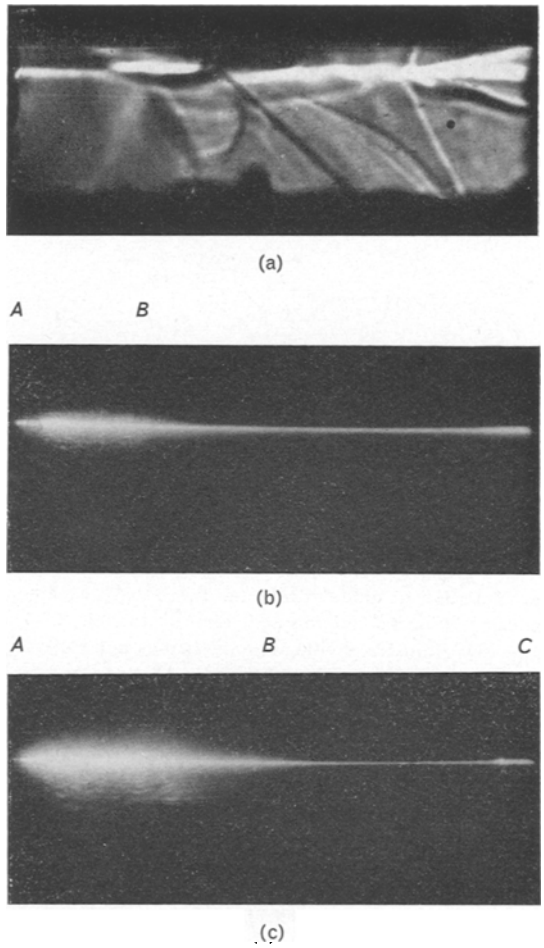

Figure 6 Infrared micrographs of diode 2613/7. (a) Transmission micrograph showing irregular, curved and intersecting, striations. (b) Emission micrograph taken just above threshold. This is a near-field radiation pattern. The laser filaments with the lowest thresholds appeared between *A* and *B*. (c) Emission micrograph taken well above threshold. The next most favoured laser filament appeared at *C*.

figs. 6b and c are near-field infrared micrographs of the diode taken above threshold. It can be seen that the strongest emission (which occurred first as the current was raised) comes from the left-hand end of the p-n junction line where there are no striations. The other laser filament occurs where a bright band (low absorption coefficient striation) intersects the p-n junction.

The correlation between emission patterns and striations is most clearly seen in microdensitometer traces as shown in fig. 7. The lower curve is a microdensitometer trace taken along the p-n junction in a micrograph of the emission (in a

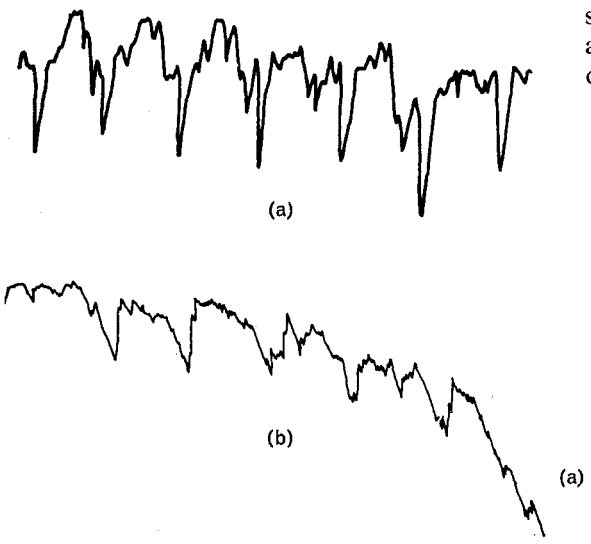

Figure 7 Microdensitometer traces taken parallel to the p-n junction of diode 2659/7. (a) Trace across a transmission infrared micrograph similar to fig. 5. The intensity of the transmitted light increases upwards. Low points therefore correspond to dark striations and high values of α. (b) Trace across a near-field emission pattern similar to fig. 4c. Emitted intensity increases upwards.

near-field radiation pattern) from a Fabry-Perot face of a diode from the same crystal as that shown in figs. 4 and 5. The upper curve is a microdensitometer trace taken along the p-n junction of a transmission infrared photomicrograph of the same face. Thus curve 7b shows the emission, and curve 7a shows the variation of infrared absorption along the p-n junction region.

3.2. Etching

On polishing the top (100) face of diode 2659/5 down to the p-n junction, and etching, broad dark lines were revealed which marked the intersections of the dark $(1\bar{1}\bar{1})$ planes with the p-n junction plane, as shown in fig. 8. By focusing the microscope up and down, it was established that these lines were actually grooves, of cusped cross-section. In addition, rows of pits were found to form a square grid. The rows of one parallel set are marked R in fig. 8. Deep grooves marked G_1 and G_2 in fig. 8 appeared to be similar to those found along active laser filaments by Abrahams *et al* [7, 8]. Grooves G_1 and G_2, however, did not occur along favoured laser filaments in diode 2659/5. The first active spots occurred to the left of B_3. At higher currents a second group of laser spots appeared between B_6 and B_7. Thus, in both cases, the laser filaments occurred near, but not at, the etched grooves.

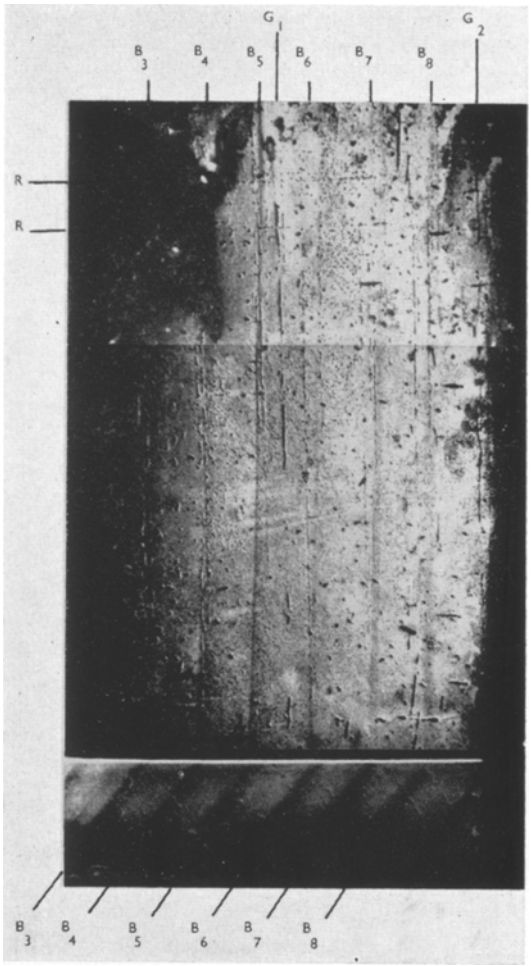

Figure 8 (a) Micrograph of the top (100) face of diode 2659/5 after polishing down to the p-n junction, and etching. Cusped grooves mark the intersections of the bands, *B*, with the p-n junction. In addition there are lines of etch pits forming a square grid and deep etch grooves marked G. (b) Emission micrograph of the front face showing the correspondence between the dark bands, *B*, and the cusped grooves on the etched p-n junction plane. Parallel rows of etch pits are marked *R*. A second set of rows are present at right angles to those marked. Deeply etched grooves also occurred parallel to the rows of pits. Two such discontinuously grooved lines are marked *G*.

The rows of etch pits, R, and grooves, G, form a square grid of spacing about 10 μm. The individual rows and grooves are aligned parallel to the two $<110>$ directions in the (100) plane.

3.3. Electron Probe Microanalysis

Abrahams *et al* [7, 8] attributed favoured laser filaments to Zn-decorated dislocations, which they believed to be responsible for the etched grooves that they found coinciding with favoured laser sites. In order to test for the presence of Zn precipitates in the p-n junction plane, electron probe microanalysis was used. Diode 2659/5, after polishing and etching as shown in fig. 8, was examined. No precipitation of tellurium (the n-type dopant), zinc (the p-type dopant), or copper (a common contaminant in semiconductors) was observed.

In order to check that this result was not due to the etchant having preferentially attacked and removed the precipitates, the observation was repeated on other diodes polished down to the p-n junction region but not etched. Again no precipitates of any of the above-mentioned elements were detected. As the sensitivity of microanalysis is rather low by semiconductor standards, this only means that any precipitates in the material must be smaller than about 0.1 μm diameter.

Precipitates were observed by transmission electron microscopy in the zinc-rich region, well into the p-type material. These precipitates, as will be shown below, however, were too small, too numerous, and too randomly distributed to be responsible for the clearly distinguishable grooves produced by etching.

Only the upper limit provided by microanalysis, therefore, applied to any precipitates occurring along the misfit dislocations that etch as continuous grooves. This is because the rarity of these defects (a few per diode i.e. per 2 mm^2) precluded their observation by electron microscopy.

3.4. Transmission Electron Microscopy

Diode 2659/5 was thinned for transmission electron microscopy in an area crossed by a dark striation. At low magnification, as shown in fig. 9, the striation appeared as a series of elongated dark areas. These were thicker areas of the film, indicating a variation of the chemical etching rate during the chemical polishing involved in thinning the specimen. This is consistent with the hypothesis that the striations are bands of varying impurity content. Fig. 9 shows the impurity content to be discontinuously distributed, even within individual striae.

Other striations examined in this way produced no effects visible in transmission electron microscopy. This presumably is due to the fact that the amplitude and the scale of the impurity segregation constituting the striations is different from one striation to another. In the latter cases the segregation was too gradual to produce any variation on a scale visible by electron microscopy. Spotty laser action occurs on an optical microscopic scale (10 to 100 μm spacings). Therefore electron microscopy provides too great a magnification to be very useful for the study of this phenomenon. In general, as fig. 9 shows, the electron micrographs of the p-n junction were unenlightening.

Figure 9 Transmission electron micrograph of an area of diode 2659/5 crossed by a striation.

As mentioned above, precipitates and diffusion-induced defects were seen in the p-type material, as shown in fig. 10. The dislocations were diffusion-induced, as the dislocation density in the n-type material, where the diffusing zinc had not penetrated, was vanishingly small on an electron microscope scale (10^4/cm^2 or less). The bowing-out of certain of the dislocations in fig. 10 between the precipitates which pin them is indicative of stress-induced glide after the precipitates had formed. That the precipitates have spherically symmetrical strain fields is shown by the characteristic two-lobe image contrast shown

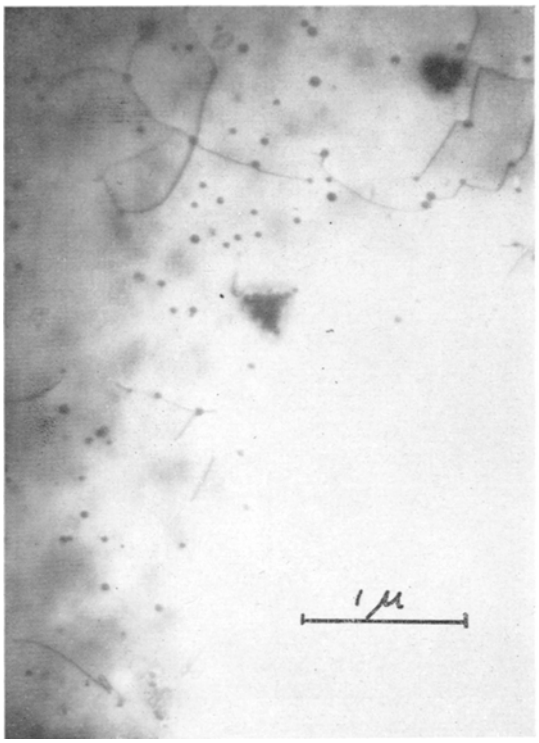

Figure 10 Transmission electron micrograph of a thin layer parallel to the p-n junction and some microns into the p-side. The diode, 2659/7, was striated and produced from the same crystal as 2659/5 (figs. 4, 5, and 8). The dots are precipitates, and diffusion-induced dislocations, some of which are pinned by precipitates, can be seen.

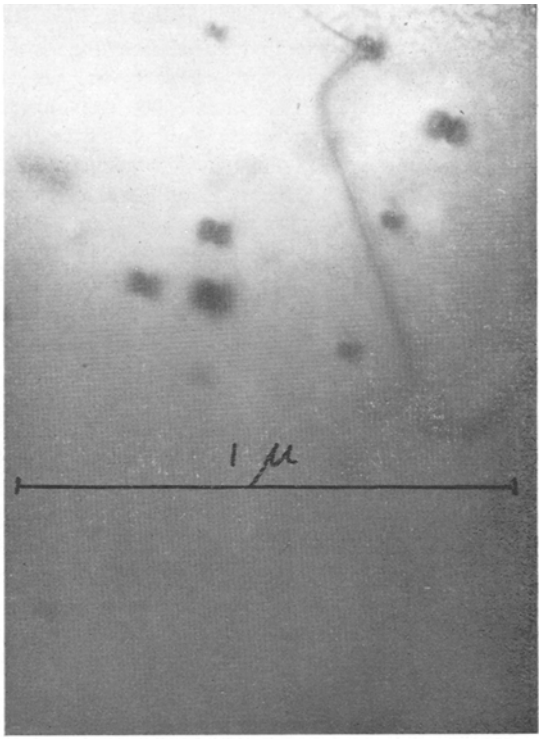

Figure 11 Transmission electron micrograph of a zinc-rich layer of a zinc-diffused, silicon-doped laser diode. The image contrast of the precipitates is that for particles with spherically symmetrical strain fields.

in fig. 11 [9]. A more detailed study of these defects will be published later.

4. Discussion

4.1. Diffusion-Induced Misfit Dislocations

The square grid of rows of etch pits, R, and grooves, G, found in the p-n junction region, as shown in fig. 8, can be ascribed to a diffusion-induced network of misfit dislocations [10].

Diffusion will lead to the introduction of dislocations when the elastic stresses, resulting from the difference in size ("misfit") between the dopant atoms and the atoms that they replace, exceed the critical stress for plastic deformation. Slip then occurs and "diffusion-induced misfit dislocations" are introduced into the vicinity of the diffusion front. This phenomenon only occurs in the case of semiconductors doped to very high, degenerate levels, of the order of 10^{19} impurity/atoms cm^3 by diffusion, with atoms of large misfit. It has been extensively studied in silicon [10, 11] and in the case of Zn diffused into GaAs, diffusion-induced slip has been observed using an X-ray topographic technique [12].

The misfit dislocation networks produced at the diffusion front consist essentially of edge dislocations oriented with their extra half-planes of atoms in the material of the smaller lattice parameter. The misfit dislocations are so spaced and aligned as to enable $N + 1$ atom planes of smaller parameter material to match up to N atom planes of the larger lattice parameter material. From crystal models, therefore, predictions of the orientations, the Burgers vectors and the spacings of the dislocations in the networks can be obtained [10]. The misfit dislocations in a (100) diffusion front should lie along the two $<110>$ directions in the plane as observed.

The spacing of misfit dislocations in a (100) heterojunction or abrupt p-n junction is given by [10]

$$p = \frac{\lambda_1 \lambda_2}{\sqrt{2}(\lambda_1 - \lambda_2)} \qquad (1)$$

where λ_1 and λ_2 are the lattice parameters on the

two sides of the junction, and may be obtained as follows. The number of atoms/cm^3 in GaAs is 4.4×10^{22}. Thus there are 2.2×10^{22} Ga atoms/cm^3. In the diodes studied here, about 2×10^{18} Te atoms/cm^2 are substituted for As atoms on both the p- and n-sides, and about 10^{19} Zn atoms/cm^3 are substituted for Ga atoms on the p-side. (The latter value is that at the knee of the Zn diffused profile) [13]. The tetrahedral covalent radii of Te, Ga, Zn, and As are 1.32 Å, 1.26 Å, 1.31 Å, and 1.18 Å respectively. Hence the average radius of atoms on the Ga and the As sublattices on each side of the junction may be obtained assuming that Vegard's Law applies. Adding these values gives the average interatomic distance, d_1 and d_2, on either side of the junction. The lattice parameters are then given by $\lambda = 4d/\sqrt{3}$. Substituting into equation 1 then gives the spacing of the misfit dislocations as $p = 10$ μm which is in excellent agreement with the observed spacing of the rows of etch pits, R, e.g. in fig. 8.

There is an apparent conflict between the etching and the transmission electron microscope results. Etching reveals a square grid of dislocations aligned with the <1 1 0> directions in the (1 0 0) plane, and spaced 10 μm apart. Transmission electron microscopy reveals tangled, non-aligned dislocations spaced a micron or less apart. The difference arises through the different resolving powers of the two techniques, and the fact that they have in consequence been applied to different regions of the diodes. Transmission electron microscopy has much the greater resolving power and shows a large density of both dislocations and precipitates to be present in the p-type Zn-diffused material. Etching of this material produces uniformly and densely stippled surfaces in which nothing can be resolved. Etching surfaces near the p-n junction, however, does not produce the dense stippling and resolvable patterns such as that in fig. 8 appear. In this region, transmission electron microscopy produces excessive magnification and can only examine excessively thin layers. Consequently the misfit dislocation networks have not been seen by this technique and most transmission electron micrographs of the p-n junction region are empty.

Thus we may conclude from the etching and electron microscope evidence that misfit dislocation networks of the form predicted by elementary crystallographic considerations [10] occur near the p-n junction and are revealed by etching. At lesser depths of diffusion, that is in the p-type region, much higher densities of irregularly arranged dislocations occur together with precipitates. These diffusion-induced dislocations are introduced by plastic slip, as has been observed in Zn-diffused GaAs by an X-ray topographical technique [12]. Far more dislocations result from this plastic deformation than the small number required for the misfit dislocation network at the diffusion front. This is just what is found to happen also in the analogous case of plastic bending [14]. Moreover a similar apparent disagreement exists in the case of diffusion-induced dislocations in silicon, between the transmission electron microscope observations and the studies made by lower magnification techniques. (This work was reviewed in [10] and subsequent work is contained in [11].)

In the case of misfit dislocations in interfaces produced by epitaxial growth, as for example in the case of the lasers studied by Abrahams and Pankove [8], geometrical complications due to the role of plastic deformation in providing the necessary dislocations should be largely or completely absent. Thus the fact that good agreement with the predictions of the simple model is obtained not only in the present case in which the misfit dislocations are diffusion-induced, but also in the case of epitaxially grown laser diodes, lends strong support to the interpretation of the observed rows of pits and grooves as being due to misfit dislocations.

The conditions that are necessary in order to produce diffusion-induced misfit dislocations are not clear. Black and Jungbluth [15] examined material prepared with rather lower temperatures of diffusion (800 to 1000° C for 2 h) than that used for the diodes examined here (1100° C for 15 min). They found no evidence for misfit dislocations. However, Schwuttke and Rupprecht did find diffusion-induced slip in GaAs slices diffused for $2\frac{1}{2}$ h at 850° C [12]. Therefore other features of the diffusion treatment such as the As vapour pressure in the container or the impurities (n-type dopants) already present in the GaAs may also help to determine whether or not diffusion does, in fact, in any particular case introduce misfit dislocations.

Only one grid of misfit dislocations contains members which etch as continuous grooves. This was observed for example in fig. 8 in which two grooves, G_1 and G_2, run perpendicular to the front and back mirror faces of the laser, but

none run parallel to these faces. It was also found by Abrahams and Pankove to be true in the case of epitaxial lasers [8]. The difference in etching behaviour between the two grids of dislocations is related to crystallographic differences between the two types of dislocation that are involved [7].

In our case, the grooves do not correlate with active laser filaments as they were found to do in epitaxial lasers [8]. This suggests that more than one type of defect can influence the laser emission pattern, but that they are not all equally effective. In the present case, in which striations and misfit dislocations were both present, the striations exerted the predominant influence. In the case of the epitaxial lasers, in which striations were not detected, the groove-producing misfit dislocations played the predominant role in relation to non-uniform laser action.

4.2. Striations

Striations, or "growth striae", are now known to be a common and significant feature of crystals grown from the melt. They arise as a result of the establishment of cyclic temperature fluctuations during growth [16, 17]. This in turn produces banded variations in the impurity content of the crystal as the growth face propagates. The striations in Czochralski-grown ("pulled") GaAs are in some cases different in origin and on a coarser scale than those in horizontal boat grown ("Bridgman" technique) material such as that studied here.

The striations constituting the fine structure inside the dark bands, as shown in fig. 5, are spaced only microns apart. The conditions required to observe them are therefore stringent. Unless the direction of viewing is parallel to the plane of the striations to within about 0.3°, then with a diode length of 2 mm, the fine striations will overlap and become indistinguishable. The striations must be accurately planar and good resolution infrared microscopy is necessary. It seems probable, therefore, that striations are often present but not observed. If the coarse striations, i.e., the dark bands, are to promote spotty laser action, the lines of intersection of the bands with the p-n junction plane must run within about 3° of the perpendicular to the Fabry-Perot mirror faces. Thus striations may sometimes be present but not so oriented as to be able to play a role in the formation of a pattern of laser filaments. Striations of this kind were found by etching in some diodes during the present investigation. The particular orientation of striations relative to the mirror faces required to affect laser action is one that can occur under a variety of circumstances, however. Ziegler and Henkel [18] observed striations in diodes of material grown by the Czochralski technique. These were convincingly shown to be the striations arising from the method of growth. The striations were found in this case also to correlate with the filamentary emission pattern*.

Striations have also been observed in boat grown GaAs by infrared Schlieren techniques and the spacing was found to be 100 μm. This spacing was found to correlate with the optimum width of lasers intended for continuous operation. The striations were therefore assumed to be responsible for the irregular distribution of laser filaments although no direct relation was established [19]. The visibility of striations in GaAs in the Schlieren arrangement is due to perodic variations of the real part of the refractive index [20].

There is direct evidence that striations affect electroluminescent emission in GaP [21] and other materials but no direct evidence of this effect, such as that in fig. 7, has been reported previously in the case of GaAs. However, Wittry [22] employed an electron probe microanalyser and found that the infrared cathodoluminescence excited by the beam exhibited striae, as did the Te doping concentration, as determined from the X-ray fluorescent radiation excited simultaneously. The infrared intensity increased as the X-ray counting rate decreased. Thus the intensity of cathodoluminescent recombination radiation increases with decrease in Te concentration.

The effect observed in the present work is a minimum emission from filaments through which the dark striations pass. Before discussing mechanisms whereby striations might influence the laser emission pattern it is necessary to consider more generally the influence of defects on lasers.

4.3. Defects and Laser Action

4.3.1. Factors Influencing Laser Action

Laser action involves the amplification, by stimulated emission, of a standing wave set up normal

*Ziegler and Henkel reported that the active filaments occurred at the places where striations intersected the p-n junction. Their figs. 6 and 7 appear to show the opposite, namely that emission is a minimum at these points, but the resolution in these micrographs is too poor for the interpretation to be unambiguous.

to the Fabry-Perot mirror faces of the diode. At threshold, gain just balances losses, that is [23, 24]

$$R\,e\,(g_t - \alpha)\,l = 1$$

where g_t is the gain per unit length at threshold, and α is the loss; l is the length of the laser normal to the mirror faces and R is the reflectivity of the mirror faces. In the case of an injection laser it can be shown that this leads to a threshold current, j_t, given by [23, 24]

$$j_t = \frac{8\pi e n_0^2\,\nu^2\,d\Delta\nu}{\eta c^2}\left[\frac{1}{l}\ln\left(\frac{1}{R}\right) + \alpha\right]$$

where e is the electron charge, n_0 is the index of refraction, ν is the frequency of the emission, $\Delta\nu$ is its line width, d is the thickness of the active region, and η is the quantum efficiency ($= T_r/T$, where T_r is the radiative lifetime, and T the total lifetime of the charge carriers).

Of the quantities involved in determining the value of the threshold current, seven are parameters of the material and could vary from place to place due to the occurrence of chemical inhomogeneities or crystalline defects. These seven parameters are n_0, ν, d, η, $\Delta\nu$, R, and α.

In addition, non-uniform distributions of current may play a role in promoting non-uniform emission. That is, features which direct current to particular areas of the p-n junction will result in the threshold being exceeded first in those areas, even if the characteristics of the material over the p-n junction are constant. A number of types of manufacturing fault can be effective in this way. Bad contacts can result in non-uniform resistance over the top and bottom of the diode. Non-uniform diffusion resulting in non-flat p-n junctions will also lead to local field enhancement and concentrated flow of junction current. Non-flat junctions are known to be harmful, and are prevented or rejected in GaAs laser manufacture [25, 26].

Precipitates threading p-n junctions, particularly at dislocations, are believed to be responsible for localised microplasma breakdown in back biased silicon p-n junctions through their effect in local enhancement of the field [27]. Localised electroluminescent emission of a similar appearance to that from silicon microplasma distributions has been observed in striated GaP [21]. Moreover, microplasma breakdown has been observed in GaAs diodes [28], and found to be associated with dislocations [29]. Thus, field enhancement by precipitates may play a role in determining the behaviour of GaAs diodes. This would provide an explanation of the observations of Abrahams and his co-workers who found enhanced laser action in filaments which etched as continuous grooves, like those marked G in fig. 5. If a row of metallic precipitates threaded the p-n junction along the groove these would result in a higher than average current through the junction along the fraction of the length of the filament that is occupied by the groove. Thus the threshold would be exceeded first in such a filament as the total diode current was increased, even if the junction characteristics, and hence the value of the threshold, were otherwise uniform throughout the diode.

There is also direct evidence that patterns of current flow through GaAs diodes can influence laser emission. Fenner used specially shaped contacts to sweep the diode current, passing in a sheet, successively through one edge of the diodes, through the middle and through the other edge. As the current swept across the diodes, laser filaments came on successively in the regions through which the current flowed [30]. Moreover magnetic fields applied so as to deflect current flow lines were found to switch emission from one active filament to another [31]. GaAs lasers with divided contacts on the p-side have been shown to have higher average threshold currents than do lasers with uniform current densities, and have useful mode control and switching properties [32].

A related phenomenon is a possible inherent instability of current flow through junctions at threshold. Nannichi [33] developed a theory in which carriers are injected across a junction at a rate inversely proportional to the square root of the lifetime in the case of carrier diffusion, and inversely as the lifetime in the case of tunnelling. When, at threshold stimulated emission begins in any filament, the lifetime is greatly reduced. This results, as Nannichi pointed out, in a further increase in the current injected into the now active filament at the expense of neighbouring filaments. Jonscher and Boyle [34] pointed out that the decrease in lifetime due to stimulated emission would alter the refractive index so as to produce a self-confining, or guiding, optical effect. These mechanisms would explain the fact that active filaments do not spread. They do not explain variations of two to one in the apparent threshold of different active filaments as shown in fig. 6, however. The latter phenomenon must

be explained in terms of the variation of the characteristics of the material from place to place over the p-n junction, or in terms of non-uniform flow of current through the diodes. The fact that the pattern of favoured laser filaments is fixed in position and reproducible in the values of the diode current at which the filaments appear also indicates that the phenomenon is structure-dependent. The phenomena contributing to filament formation due to the decrease of carrier lifetime at the onset of stimulated emission will act to exaggerate, or multiply, the apparent non-uniformity of diodes. This multiplication effect makes it difficult to carry out numerical comparisons between the values of diode current at which various filaments come on and possible variations of the material parameters. The possibility of microscopic non-uniformities of current flow, as discussed above, further contributes to this difficulty. Only order of magnitude checks on the plausibility of various possible mechanisms for filamentary laser action are therefore possible at present.

As was pointed out above, variations in seven parameters of the material could in principle contribute to the variation of the threshold from place to place. It is possible however to eliminate some of these from consideration on experimental grounds or by means of quantitative arguments as follows:

l The threshold current is inversely proportional to the distance between the mirror faces, l, but no correlation between emission patterns and surface features such as polishing scratches or cleavage steps was found here or has been reported in the literature.

Moreover, the value of l is large (2 mm) in the diodes studied here. Therefore large fractional changes in j_t, such as are required to explain the observed emission patterns, would require impossibly large absolute changes of diode length if this term were to be significant.

n_0 The threshold current is proportional to the square of the refractive index, n_0. However, the refractive index is unlikely to vary by more than about one part in a thousand across the striations [19, 20] although variations of 1 to 2% occur across p-n junctions in GaAs [40]. The variation of n_0^2 probably by less than about two parts in a thousand (and certainly less than 4%), then, is negligible in relation to the large variations possible in some of the other parameters of the material, and in relation to the large variations in apparent threshold between one active filament and another (2:1 in diode 2613/7 as shown in fig. 6).

R (reflectivity of the mirror faces) Threshold current varies as $\ln(1/R)$, which is a much lesser dependence that in the case of the other parameters of the material. Variations of R might conceivably occur across the striations due either to variation of the thickness of the surface oxide, due to an influence of doping on oxidation rate, or to the dependence of R on the refractive index. It is possible to test for any large variation of R by means of a microscopic method of measurement of R [35]. This was done. No change in R could be detected on scanning across the striations. Any such variations in R are therefore less than about 1% which is the limit of sensitivity of the technique.

In any case the large value of l means that any variations in R are relatively unimportant.

All of the remaining parameters of the material can in principle vary significantly due to the presence of chemical inhomogeneities or crystallographic defects as follows. ν, the frequency of the emitted photons is known to vary with externally applied stress [36], and will therefore also vary in the presence of internal stresses. Moreover, in the case of spontaneous cathodoluminescence from Te-doped GaAs, and of spontaneous electroluminescence from Se- and Si-doped diodes, both ν and $\Delta\nu$ are found to vary with the electron concentration [37, 38].

d, the thickness of the active, light-emitting region depends on the variation of the refractive index [39, 40], and therefore on the nature of the p-n junction, abrupt or graded, that is, on the impurity distribution profiles. η, the quantum efficiency, will vary with the densities of radiative and non-radiative recombination centres in the material. α, the absorption coefficient, varies strongly with the amount and type of doping in GaAs in conditions of both incoherent and coherent emission [41, 42].

4.3.2. Defects in Laser Diodes

A number of different types of defect have been found in GaAs lasers. These are gross non-flatnesses of the p-n junction [25] (these are sometimes associated with subgrain boundaries [26]), misfit dislocation networks in the p-n junction [7, 8, 12] as shown in fig. 8, striations [18, 19] as shown in figs. 5 and 6a, and precipitates [43], as shown in figs. 10 and 11.

All possible defects in GaAs lasers can be classified in terms of the seriousness of their

effects as follows. (i) Disastrous effects (unacceptably high thresholds or failure to lase) are produced by macroscopic defects associated with bad contacts or bad diffusion. (ii) Spotty or filamentary laser emission can only be promoted by defects that influence lines running in the p-n junction perpendicularly to the mirror faces, since, if defects are significantly to affect the threshold of a filament, they must run through a considerable fraction of its length. Moreover, such defects must be of relatively large cross-section, since the filaments are microns thick (the thickness of the active region, d [24, 39]) and have the same width (the laser spots are roughly circular). This consideration greatly limits the kinds of defects which can play a role in filamentary emission. The only defects with the required size and shape would be large needle shaped precipitates [43], dislocation lines along which rows of small precipitates have nucleated [7, 8], and lines of intersection of the p-n junction with thick planar defects, that is, with striations and perhaps with subgrain boundaries to which impurities have segregated. The latter type of defect is unlikely to promote filamentary laser action in practice, as enhanced Zn diffusion down the subgrain boundary will generally have taken place with disastrous effect [26]. Dislocation lines by themselves are unlikely to be effective as the row of dangling bands in the core has a capture cross-section only of atomic dimensions and in very heavily doped GaAs, such as that used in lasers, the space-charge cylinder round the dislocation will also be of very small radius. This conclusion is supported by the observation that only those misfit dislocations that etch as continuous grooves, and are therefore probably closely decorated with precipitates, influence emission [7, 8]. (iii) All the remaining types of defects will affect only points or small localised areas in the p-n junction plane. These types of defect include dislocation lines or needle-like precipitates threading the junction, and small clusters of point defects. Such defects may be expected to produce fluctuations in the value of the laser threshold current from point to point, and will statistically modify the overall device characteristics, and therefore will play a role in determining device yield in production runs.

4.4. Striations and Laser Action

The defects that were found actually to influence emission in the lasers studied here were striations. The mechanism whereby this influence is exerted might involve any one of several properties of the material as discussed above. Certain of these general possibilities can, however, be eliminated in the particular case of striations on the grounds of the sign of the effect as follows.

The basic observation is that, as figs. 4, 6, and 7 show, dark striations correspond to inactive filaments and light striations to active filaments. That is, dark striations correspond to high values of the threshold. But dark striations are regions of high absorption coefficient and high absorption corresponds to low levels of Te doping [40-42]. This is true for the case of band gap radiation and an average doping level of 1 to 3×10^{18} Te atoms/cm^3, with which we are here concerned. Thus, low Te concentrations correspond to high values of the threshold current.
But

$$j_t = \frac{8\pi e n_0 \nu^2 d \Delta\nu}{\eta c^2}\left[\frac{1}{l}\ln\left(\frac{1}{R}\right) + \alpha\right]$$

that is, j_t, the threshold current, is proportional to $\Delta\nu$, and inversely proportional to η. But $\Delta\nu$ decreases with decrease of Te concentration in the cases both of cathodoluminescence [37], and p-n junction injection electroluminescence [38]. The variation of $\Delta\nu$ with Te concentration would therefore tend to lower the threshold in the dark bands, contrary to the observed facts. Similarly, the intensity of cathodoluminescent emission, and hence η, increases with decrease of Te concentration [22]. The variation of η on this evidence, too, would favour laser action in the dark bands contrary to observation. This leaves α, ν and d to be considered quantitatively.

What has been observed is the value of the total current through the diode at which filaments come on whereas j_t is the local value of the threshold current in the filaments. Thus we may write

$$MI_{AV} = j_t$$

where I_{AV} is the total current divided by the area of the p-n junction, and M is a multiplying factor to take into account any channelling of current into the filament under consideration by macroscopic inhomogeneities, such as non-uniform contact resistances to the diode, non-uniform resistivities in either the p- or the n-type material, or field enhancing local features in the junction. In addition a local multiplying factor, m, would have to be included when comparing neighbouring filaments due to the tendency of all the charge carriers within a distance of about L (the charge

carrier diffusion length) to diffuse into an active filament [33].

What has been determined experimentally is that the values of I_{AV} at which active filaments begin to lase, differ by factors of 2 or 3, while the values of I_{AV} at which inactive filaments in dark striations come on are still higher, as these filaments are still not lasing at the largest currents the diode can take. The variation of M and j_t will be considered separately.

4.4.1. Variation of Threshold Current due to Variation in Properties of the Material

As shown above, three properties of the material have to be considered: α, ν, and d.

There is direct evidence that ν varies from one active filament to another in GaAs lasers. Raab *et al* [44] used a movable slit to pass the light from one filament at a time from a striated Te-doped GaAs laser. The emission spectra of the separate spots was examined, and it was found that the frequencies of the lines emitted varied by a few per cent. It was suggested that this frequency variation was due to the impurity concentration variation across the striations. However it is clear that a variation of a few per cent in ν will not suffice to explain variations in j_t by a factor of 2 or 3. Moreover, even variations of a few per cent are larger than those that are generally found (C. H. Gooch*, private communication).

Much larger variations of α are probable, and larger variations of d are possible than those of ν. A change of Te concentration from 2×10^{18} to $4.6 \times 10^{18}/cm^3$ changes the absorption coefficient α of GaAs by a factor of about four [41]. The thickness of the active region, d, is 1 to 3 μm [24]. However, it has been found that the active regions for different spontaneous emission peaks differ in thickness, being more than a micron thick for the voltage insensitive features of the spectrum, and 600 Å or less thick for the band-filling recombination radiation [45].

Both α and d will, in fact, vary across the striations. The variation of α is an immediate consequence of the variation of the impurity concentration. The fact that the striations were readily visible in both emission and transmission micrographs was due to the considerable variations in α that were present in the samples. The variation of d across the striations follows from the fact that the refractive index of the material varies across the striations [19, 20]. The width of the active region is determined by the variation in the refractive index across the p-n junction region [39, 40]. It is possible that very small variations in the background of the refractive index of the n-type material due to the striations, might therefore produce disproportionate variations in the value of d. This effect of refractive index changes would be indirect. It was shown in section 4.3. above, that the variations of the refractive index n_0 were too small to account directly for the observed variations in the threshold current from filament to filament.

The variations in α therefore readily suffice to account for the observed variations in the threshold currents of the active filaments although variations in d might be significant.

Variations in α were directly observed and found to correlate with emission patterns. It is also clear that the variations in α can be quite large enough to account on their own for the experimental observations. Possible variation in d, therefore, is an unnecessary hypothesis, and it is likely that the principle factor in promoting filamentary laser action in the diodes examined here is the variation of the absorption coefficient across the striations due to the non-uniform impurity distribution which they represent.

4.4.2. Variation of Current from Filament to Filament due to Channelling

The possibility of current channelling has been shown in the previous section to be unnecessary for the explanation of the observed variations in the total diode current corresponding to individual filament thresholds. However, it is known that deflection of current flow patterns through lasers by external means can suffice to turn filaments on and off [30, 31]. The possibility that current channelling down the striations occurs must therefore be considered.

Conductivity varies approximately linearly with dopant concentration in the extrinsic range. But the absorption coefficient varies much more rapidly (and more complicatedly) than the first power of the impurity concentration [41]. Thus the absorption coefficient (and, possibly, the thickness of the active region, d) will produce much larger fractional changes in j_t than the variations of M produced by the striations. Current channelling by the striations may however, play some part in the observed phenomenon

*Address: Services Electronics Research Laboratory, Baldock, Herts, UK.

since the sign of the effect is right, as the following argument shows. The dark bands, as demonstrated previously, correspond in the present experimental circumstance to low Te concentrations, and therefore to low electrical conductivities, and low current densities. The dark bands were in fact observed to correspond to minimal emission, as is to be expected on this basis.

Non-uniform distributions of current across the p-n junctions might also arise from electric field enhancing corrugations in striated diodes. The rise and fall of tellurium concentration across the striations implies a shift of the position of the p-n junction in the form of saw-toothed corrugations.

5. Conclusions

(i) Several different types of defects (striations, dislocations, subsurface damage [43] and large scale segregation [43]) can be simultaneously present in GaAs. Several different techniques must therefore be used together to get a complete picture of the structural defects and inhomogeneities in lasers, or any other form of GaAs device or material.

(ii) A considerable number of the properties of the material that enter into the expression for the threshold current for stimulated emission can vary by large factors in the presence of defects, and/or chemical inhomogeneities. Measurements of overall device performance parameters (especially as a function of variations in device preparation techniques such as crystal growth and diffusion) are therefore of little value unless the lasers tested have been shown to be microscopically homogeneous. The degree of homogeneity and perfection required by certain aspects of the theory may in fact be currently unattainable. Irreproducibility, high rejection rates and large changes in device performance due to changes in preparation techniques are all typical of GaAs laser production. Studies of localised laser performance in relation to local conditions of purity and perfection are therefore desirable.

(iii) Striations probably influence the value of the threshold current mainly through the variations they cause in α, the infrared absorption coefficient.

Acknowledgements

It is a pleasure to thank Mr S. H. Levene for his co-operation in some of the etching observations, and Dr D. G. Murchison for allowing us to use his equipment for the measurement of R. Thanks are due, too, to Professor J. G. Ball for the provision of research facilities. This work was done under a CVD contract and is published by permission of the Ministry of Defence (Navy Department).

References

1. R. F. BROOM, C. H. GOOCH, C. HILSUM, and D. J. OLIVER, *Nature* **198** (1963) 368.
2. R. N. HALL, *Solid State Electronics* **6** (1963) 405.
3. G. E. FENNER and J. D. KINGSLEY, *J. Appl. Phys.* **34** (1963) 3204.
4. M. S. ABRAHAMS and C. J. BUIOCCHI, *ibid* **36** (1965) 2855.
5. D. B. HOLT, R. PORTER, and B. A. UNVALA, *J. Sci. Instr.* **43** (1966) 371.
6. M. J. HILL, B. A. UNVALA, and D. B. HOLT, *ibid Ser. 2* **1** (1968), to be published.
7. M. S. ABRAHAMS and C. J. BUIOCCHI, *J. Appl. Phys.* **37** (1966) 1973.
8. M. S. ABRAHAMS and J. I. PANKOVE, *ibid* **37** (1966) 2596.
9. M. F. ASHBY and L. M. BROWN, *Phil. Mag.* **8** (1963) 1083.
10. D. B. HOLT, *J. Phys. Chem. Solids* **27** (1966) 1053.
11. E. LEVINE, J. WASHBURN, and G. THOMAS, *J. Appl. Phys.* **38** (1967) 81, 87.
12. G. H. SCHWUTTKE and H. RUPPRECHT, *ibid* **37** (1966) 167.
13. F. A. CUNNEL and C. H. GOOCH, *J. Phys. Chem Solids* **15** (1960) 127.
14. R. L. BELL and A. F. W. WILLOUGHBY, *J. Matls. Sci.* **1** (1966) 219.
15. J. F. BLACK and E. D. JUNGBLUTH, *J. Electrochem. Soc.* **114** (1967) 188.
16. D. T. J. HURLE, *Phil. Mag.* **13** (1966) 305.
17. D. T. J. HURLE, J. GILLMAN and E. J. HARP, *ibid* **14** (1966) 205.
18. G. ZIEGLER and H.-J. HENKEL, *Z. angew. Phys.* **19** (1965) 401.
19. H. SALOW and K.-W. BENZ, *ibid p.* 157.
20. M. E. DROUGARD, *J. Appl. Phys.* **37** (1966) 1858.
21. M. GERSHENZON and A. A. ASHKIN, *ibid* p. 246.
22. D. B. WITTRY, *Appl. Phys. Letters* **8** (1966) 142.
23. G. J. LASHER, *I.B.M. J. Res. and Devel.* **7** (1963) 58.
24. M. I. NATHAN, *Appl. Optics* **5** (1966) 1514.
25. J. C. MARINACE, *J. Electrochem. Soc.* **110** (1963) 1153.
26. D. A. SHAW, K. A. HUGHES, N. F. B. NEVE, D. V. SULWAY, P. R. THORNTON, and C. GOOCH, *Solid State Electronics* **9** (1966) 664.
27. W. SHOCKLEY, *ibid* **2** (1960) 35.
28. R. A. LOGAN, A. G. CHYNOWETH, and B. G. COHEN, *Phys. Rev.* **128** (1962) 2518.
29. J. P. MCARTHY, *J. Appl. Phys.* **37** (1966) 436.
30. G. E. FENNER, *ibid* p. 4991.
31. A. B. FOWLER and E. J. WALKER, *ibid* **35** (1964) 727.

32. M. I. NATHAN, J. C. MARINACE, R. F. RUTZ, A. E. MICHEL, and G. J. LASHER, *ibid* **36** (1965) 473.
33. Y. NANNICHI, *ibid* **37** (1966) 3009.
34. A. K. JONSCHER and N. H. BOYLE, "Gallium Arsenide" (I.P. and P.S. Conference Series No. 3) (Institute of Physics and the Physical Society, London, 1967) p. 78.
35. J. M. JONES and D. G. MURCHISON, *Nature* **205** (1965) 663.
36. The literature on the effects of stress is reviewed in P. T. LANDSBERG, *Solid State Electronics* **10** (1967) 516, 517, and 529.
37. H. C. CASEY and R. H. KAISER, *J. Electrochem. Soc.* **114** (1967) 149.
38. R. BRAUNSTEIN, J. I. PANKOVE, and H. NELSON, *Appl. Phys. Letters* **3** (1963) 31.
39. R. C. C. LEITE and A. YARIV, *Proc. IEEE* **51** (1963) 1035.
40. J. E. LUDMAN and K. M. HERGENROTHER, *Solid State Electronics* **9** (1966) 863.
41. D. E. HILL, *Phys. Rev* **133** (1964) A866.
42. R. HUNSPERGER and J. BALLANTYNE, *Appl. Phys. Letters* **10** (1967) 130.
43. B. D. CHASE and D. B. HOLT, *J. Matls. Sci.* **3** (1968) 178.
44. S. RAAB, H. BACHERT, and A. KEIPER, *Phys. Stat. Solidi* **19** (1967) K59.
45. H. C. CASEY, R. J. ARCHER, R. H. KAISER, and J. C. SARACE, *J. Appl. Phys.* **37** (1966) 893.